Electronic Supplementary Information (ESI) for

Fabrication of Hierarchical Porous Carbon Frameworks from Metal-Ion-Assisted Step-Activation of Biomass for Supercapacitors with Ultrahigh Capacitance

Chengshuai Chang,[†,‡] He Wang,[†] Yunqiang Zhang,[†] Shulan Wang,*[,†] Xuan Liu*[,†] and Li Li*[,‡]

† Department of Chemistry, School of Science, Northeastern University, Wenhua Road, Heping District, Shenyang 110819, P. R. China

‡ School of Metallurgy, Northeastern University, Wenhua Road, Heping District, Shenyang 110819, P. R. China

Address all correspondence to the author.

*Email: slwang@mail.neu.edu.cn (Shulan Wang); xuanliucmu@gmail.com (Xuan Liu); lilicmu@alumni.cmu.edu, lilicmu@gmail.com (Li Li)

Number of Pages: 13
Number of Figures: 5
Number of Tables: 5

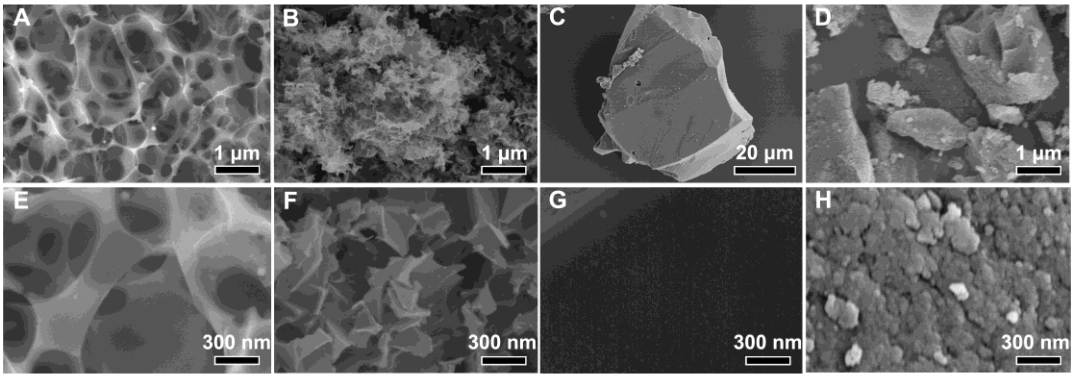

Fig. S1 SEM images of (A, E) KCPF; (B, F) NCPF; (C, G) ZCPF and (D, H) PCPF.

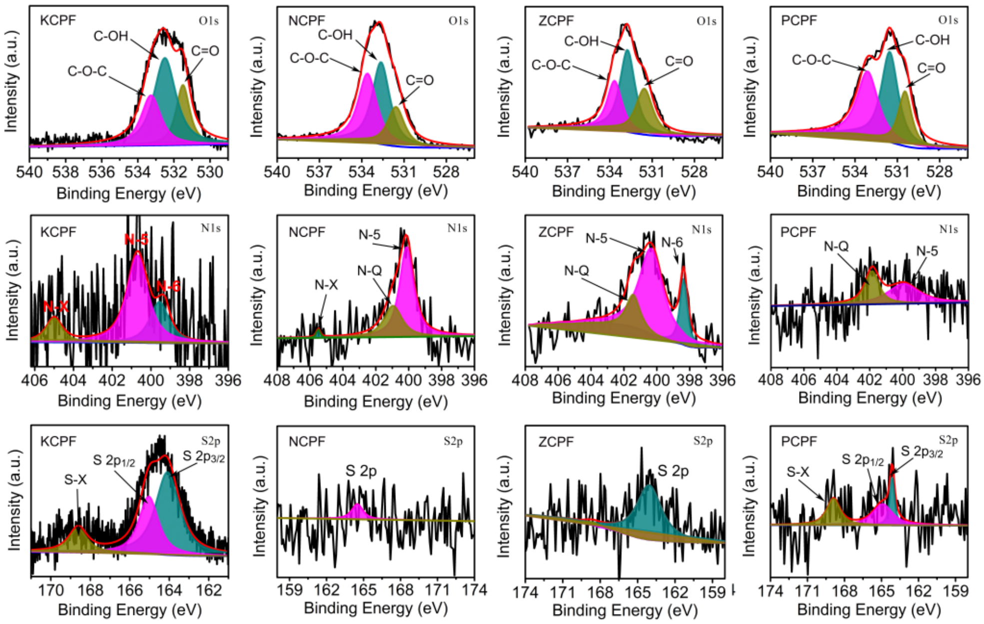

Fig. S2 High-resolution XPS scans for N 1s, O 1s and S 2p of KCPF, NCPF, ZCPF and PCPF.

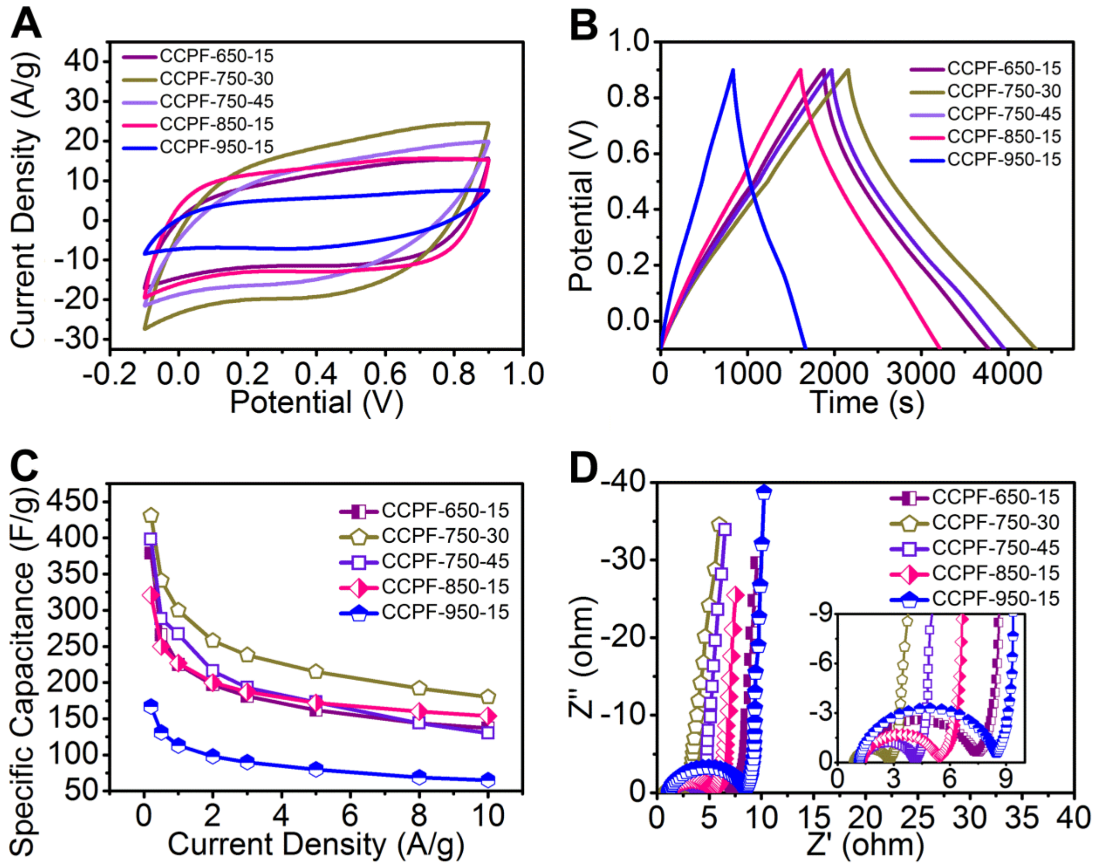

Fig. S3 Electrochemical performance of CO_2 activated samples in 2 M H_2SO_4 solution in a three-electrode system: (A) CVs at a scan rate of 100 mV s^{-1}; (B) GCD curves at the current density of 0.2 A g^{-1}; (C) Specific capacitance at different current densities and (D) Nyquist plots.

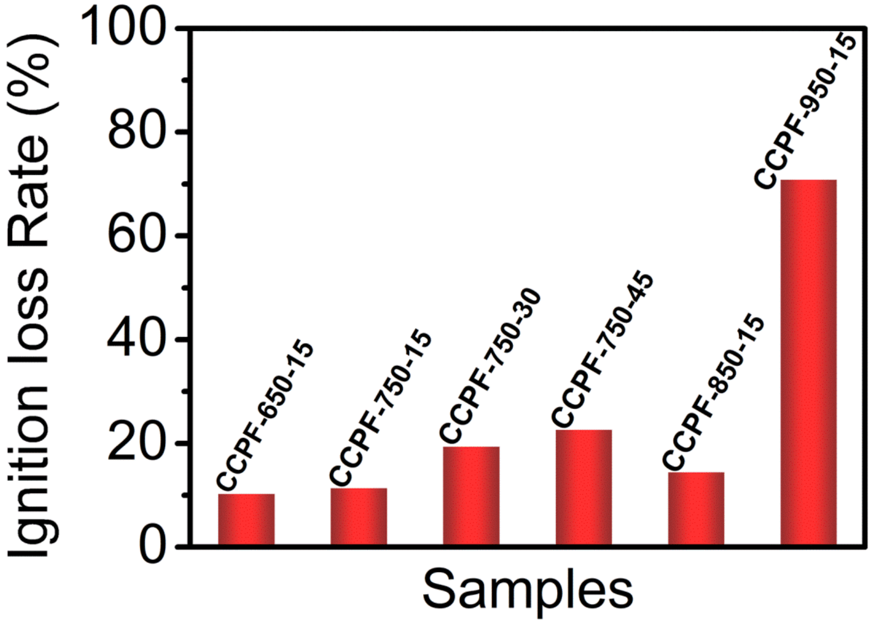

Fig. S4 Ignition loss rate of CO_2 activated samples.

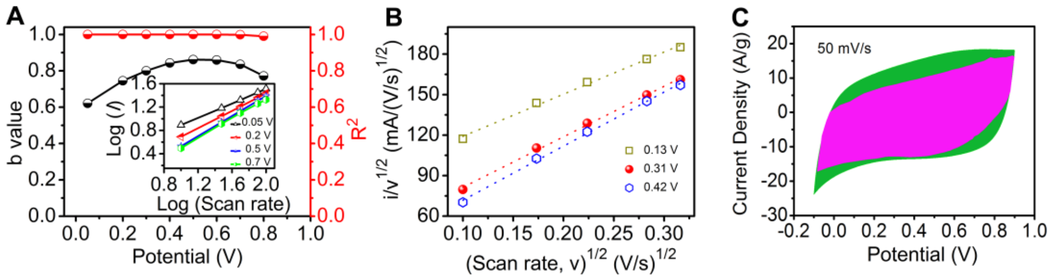

Fig. S5 CCPF-750-15 in 2 M H_2SO_4 electrolyte (A) b value against voltage. The inset is the plots of current response against scan rate at different voltages; (B) Plots of $i/v^{1/2}$ vs. $v^{1/2}$ for calculating k_1 and k_2; (C) capacitive contribution of surface controlled (magenta) and diffusion-controlled (green) at 50 mV/s.

Table S1 Element C, O, N and S content (atom%) obtained from XPS.

The as-prepared samples	Element content (atom%)			
	C	**O**	**N**	**S**
KCPF	84.93	11.82	1.50	1.75
NCPF	87.91	10.84	0.97	0.27
ZCPF	86.99	9.98	2.52	0.51
PCPF	87.33	10.53	1.40	0.74
CCPF-750-15	86.67	10.24	1.37	1.72

Table S2 The detailed information of the reported biochar sample.

Precursor	**Treatment conditions**	**SSA (m^2/g)**	**Electrolyte**	**Capacitance (F/g)**
Tobacco rods	Hydrothermal carbonization/KOH activation	2115	6 M KOH	287 (0.5 A/g)
Glucose@rice straw	In situ decoration/KOH activation	1122	6 M KOH	337 (1.0 A/g)
Rice husk	Pre-carbonization/MgO, CTP, KOH activation	3120	6 M KOH	315 (0.1 A/g)
Rice straw	Carbonization/KOH activation	1007	1 M H_2SO_4	332 (0.5 A/g)
Cotton stalk	KOH-chemical activation	1964	1 M H_2SO_4	242 (1.0 A/g)
Pomelo peel	Carbonization	2725	6 M KOH	342 (0.2 A/g)
Poplar catkins	Carbonization/$ZnCl_2$ activation	1463	1 M H_2SO_4	251 (0.5 A/g)
Chitosan	Aerogel formation/ carbonization/activation	2435	6 M KOH	197 (0.2 A/g)
Human hair	carbonization	1306	6 M KOH	340 (1.0 A/g)
Chinese parasol fluff	Metal ion pre-treatment/ two-step post-activation	1449	2 M H_2SO_4	682 (0.2 A/g)

Table S3 Comparison of the electrochemical properties of the as-made samples with other biomass carbon from recent references.

Precursor	C_g (F/g)	Measurements done at	Current density (A/g)/cycle number/C_g retention (%)	References
Commercial cotton	305	0.1 A/g	5/10000/98	1
Bamboo char	222	0.5 A/g	------------	2
Perilla frutescens	270	0.5 A/g	2/10000/96.1	3
Sugar cane bagasse	300	0.25 A/g	2/5000/90	4
Salvia splendens	294	1 A/g	2/20000/92.5	5
Willow catkin	285	1 A/g	5/10000/98	6
Poplar catkins	251	0.5 A/g	20/10000/99.5	7
Cattle bones	258	5 A/g	10/5000/96.4	8
Banana fibers	74	0.5 A/g	0.5/500/89	9
Pomelo peel	342	0.2 A/g	10/1000/98	10
Tufo	262	0.5 A/g	3/10000/102	11
Cotton	175	1 A/g	20/5000/95	12
Lotus stems	174	5 mV/s	1/10000/72	13
CCPF-750-15	682 397	0.2, 1 A/g	10/10000/92.19	This work

Table S4 R_{ct} and R_s values of the as-prepared samples.

Samples	$\boldsymbol{R_{ct}}$ **(Ω)**	$\boldsymbol{R_s}$ **(Ω)**
CCPF-650-15	6.25	1.26
CCPF-750-30	1.78	0.96
CCPF-750-45	2.88	1.31
CCPF-850-15	4.06	1.37
CCPF-950-15	7.32	1.21

Table S5 The detailed information of the reported biochar sample.

Precursor	Treatment conditions	SSA (m^2/g)	Electrolyte	Energy density (Wh/kg)	Power density (W/kg)
Glucose@rice straw	In situ decoration /KOH activation	1122	6 M KOH	9.3	500
Pomelo peel	Carbonization	2725	6 M KOH	9.4	96
Leonardite fulvic acid	Solvent exchange/activation process	2807	6 M KOH	13	60
Sodium alginate	polymerization carbonization/activation	1695	H_2SO_4-PVA gel	3.8	246
Bamboo char	K_2FeO_4/carbonization	1732	KOH-PVA gel	6.68	100
Prawn shells	Carbonization/KOH activation	1606	1 M H_2SO_4	6.5	1000
Apricot shell	TIPS approach KOH activation	1790	1 M H_2SO_4	5.1	4150
Peanut shell	$ZnCl_2$ activation	1552	1 M Et_4NBF_4/PC	19.3	1007
Willow catkins	Carbonization KOH activation	1776	1 M $LiPF_6$	37.9	700
Sodium lignosulfonate	Thermostabilization carbonization	1939	1 M $SBPBF_4$/PC	29.3	2000
Rice straw	Carbonization KOH activation	1007	[EMIM][BF_4]	17.4	126
Carboxymeth -ylcellulose sodium	KNO_3 activation	1773	1 M $TEASF_4$/AN	34.7	675
Birch wood	Carbonization NaOH activation	1456	1 M $(C_2H_5)_4NBF_4$/AN	23.25	3600
Chinese parasol	Metal ion pre-treatment/	1449	2 M H_2SO_4	17.64	100
fluff	two-step post-activation		1M $BMIMBF_4$/AN	46.38	300

References

1 Fan, M.; Song, L.; Li, X.; Fan, L. Assembly of Graphene Aerogels into the 3D Biomass-Derived Carbon Frameworks on Conductive Substrates for Flexible Supercapacitors. *Carbon* **2017**, *111*, 658–666.

2 Gong, Y.; Li, D.; Luo, C.; Fu, Q.; Pan, C. Highly Porous Graphitic Biomass Carbon as Advanced Electrode Materials for Supercapacitors. *Green Chem.* **2017**, *19*, 4132–4140.

3 Liu, B.; Liu, Y.; Chen, H.; Yang, M.; Li, H. Oxygen and Nitrogen Co-Doped Porous Carbon Nanosheets Derived from Perilla Frutescens for High Volumetric Performance Supercapacitors. *J. Power Sources* **2017**, *341*, 309–317.

4 Rufford, T.E.; Hulicova-Jurcakova, D.; Khosla, K.; Zhu, Z.; Lu, G.Q. Microstructure and Electrochemical Double-Layer Capacitance of Carbon Electrodes Prepared by Zinc Chloride Activation of Sugar Cane Bagasse. *J. Power Sources* **2010**, *195*, 912–918.

5 Liu, B.; Yang, M.; Chen, H.; Liu, Y.; Yang, D.; Li, H. Graphene-Like Porous Carbon Nanosheets Derived from Salvia Splendens for High-Rate Performance Supercapacitors. *J. Power Sources* **2018**, *397*, 1–10.

6 Li, Y.; Wang, G.; Wei, T.; Fan, Z.; Yan, P. Nitrogen and Sulfur Co-Doped Porous Carbon Nanosheets Derived from Willow Catkin for Supercapacitors. *Nano Energy* **2016**, *19*, 165–175.

7 Gao, S.; Li, X.; Li, L.; Wei, X. A Versatile Biomass Derived Carbon Material for Oxygen Reduction Reaction, Supercapacitors and Oil/Water Separation. *Nano Energy* **2017**, *33*, 334–342.

8 Niu, J.; Shao, R.; Liang, J.; Dou, M.; Li, Z.; Huang, Y.; Wang, F. Biomass-Derived Mesopore-Dominant Porous Carbons with Large Specific Surface Area and High Defect Density as High Performance Electrode Materials for Li-ion Batteries and Supercapacitors. *Nano Energy* **2017**, *36*, 322–330.

9 Subramanian, V.; Luo, C.; Stephan, A.M.; Nahm, K.S.; Thomas, S.; Wei, B. Supercapacitors from Activated Carbon Derived from Banana Fibers. *J. Phys. Chem. C* **2007**, *111*, 7527–7531.

10 Liang, Q.; Ye, L.; Huang, Z.-H.; Xu, Q.; Bai, Y.; Kang, F.; Yang, Q.-H. A Honeycomb-Like Porous Carbon Derived from Pomelo Peel for Use in High-Performance Supercapacitors. *Nanoscale* **2014**, *6*, 13831–13837.

11 Ouyang, T.; Cheng, K.; Yang, F.; Zhou, L.; Zhu, K.; Ye, K.; Wang, G.; Cao, D. From Biomass with Irregular Structures to 1D Carbon Nanobelts: a Stripping and Cutting Strategy to Fabricate High Performance Supercapacitor Materials. *J. Mater. Chem. A* **2017**, *5*, 14551–14551.

12 Wang, H.; Yi, H.; Zhu, C.; Wang, X.; Fan, H.J. Functionalized Highly Porous Graphitic Carbon Fibers for High-Rate Supercapacitive Electrodes. *Nano Energy*, **2015**, *13* 658–669.

13 Zhang, Y.; Liu, S.; Zheng, X.; Wang, X.; Xu, Y.; Tang, H.; Kang, F.; Yang, Q.; Luo, J. Biomass Organs Control the Porosity of Their Pyrolyzed Carbon. *Adv. Funct. Mater.* **2017**, *27,* 1604687–1604694.